Supplementary Information for

Niobium grafted mesoporous silica for production of biorenewable *p*-xylene from concentrated 2,5-dimethylfuran

Yi Zhao, Kai-Zhi Wang, Ze-Hui Sun, Qi Zhang, Zi-Jian Wang, Yong-Mei Liu, He-Yong He, and Yong Cao*

** Corresponding author, E-mail address: yongcao@fudan.edu.cn*

Department of Chemistry, Shanghai Key Laboratory of Molecular Catalysis and Innovative Materials, Fudan University, Shanghai 200433, P. R. China.

Contents

Supplementary Information

1. Materials and Chemicals

Niobium(V) ethoxide ($Nb(OC_2H_5)_5$, 99.999%), niobium(V) chloride ($NbCl_5$, 99.95%), niobium(V) oxalate hydrate (19.9 wt% Nb_2O_5) was supplied by Alfa Aesar. Niobium(Ⅴ) oxide (Nb_2O_5, 99.5%), toluene (C_7H_8, 99.5%), ethanol (C_2H_5OH, 99.7%), 1,4-dioxane ($C_4H_8O_2$, 99.5%), tetrahydrofuran (C_4H_8O, 99.5%), *n*-heptane (C_7H_{16}, 99.0%), cyclohexane (C_6H_{12}, 99.0%), *p*-xylene (C_8H_{10}, 99.5%), cetyl-trimethylammonium bromide (CTAB, 99.0%), 1,3,5-trimethylbenzene (TMB, 99.5%), pyridine (C_5H_5N, 99.5%), naphthalene ($C_{10}H_8$, 99.5%), acetone (C_3H_6O, 99.5%), phosphoric acid (H_3PO_4, 85%), hydrochloric acid (HCl, 37%), nitric acid (HNO_3, 65%), hydrofluoric acid (HF, 40%), oxalic acid dihydrate ($H_2C_2O_4 \cdot 2H_2O$, 99.5%), sodium hydroxide (NaOH, 99.0%) were supplied by Sinopharm. 2,5-Dimethylfuran (DMF, 99%), 2,5-hexanedione (HDO, 97%), 3,6-dimethyl-2-cyclohexenone ($C_8H_{12}O$, 95%), 2,5-dihydrofuran (C_4H_6O, 98%), dodecylamine ($C_{12}H_{27}N$, 99%), tetraethyl orthosilicate (TEOS, 99%), dodecyl-trimethylammonium bromide ($C_{15}H_{34}BrN$, 99%), trimethyl-octadecylammonium bromide ($C_{21}H_{46}BrN$, 99%), tetraethylammonium hydroxide (TEAOH, 25 wt% and 35 wt% solution in H_2O), niobium(V) oxalate hydrate ($C_{10}H_5NbO_{20} \cdot xH_2O$, 19.2 wt% Nb), 2-methoxyethanol ($C_3H_8O_2$, 99%), titanium (IV) isopropoxide ($Ti[OCH(CH_3)_2]_4$, 98%), potassium niobate ($KNbO_3$, 99.999%), tantalum(V) ethoxide ($Ta(OC_2H_5)_5$, 99.99%), ammonium metatungstate hydrate ($(NH_4)_6H_2W_{12}O_{40} \cdot xH_2O$, 99.9%), 2-methylfuran (C_5H_6O, 99%), furan (C_4H_4O, 99%) were obtained from J&K Chemicals. Maleic anhydride ($C_4H_2O_3$, 99.5%), 2,3-dimethyl-1,3-butadiene (C_6H_{10}, 98%) and cyclohexanol ($C_6H_{12}O$, 98%) were supplied by Aladdin Reagents.

1-Methyl-3-propylbenzene ($C_{10}H_{14}$, 99%), vanadium(V) tri-*i*-propoxy oxide ($VO(OC_3H_7)_3$, 97.0%) were acquired from TCI Chemicals. Zirconium(V) hydroxide ($Zr(OH)_4$, 97%), ammonium metatungstate(VI) hydrate ($(NH_4)_6H_2W_{12}O_{40} \cdot xH_2O$), sodium silicate solution ($Na_2O(SiO_2)_x \cdot xH_2O$, 27 wt% SiO_2), cetyltrime- thylammonium chloride solution (CTAC, 25 wt% in H_2O), yttrium(III) tris(isopropoxide) ($C_9H_{21}O_3Y$, 99.99%), Pluronic P123 ($EO_{20}PO_{70}EO_{20}$, average Mn ~5800) were supplied by Sigma-Aldrich. Ethylene (99.99%), helium (99.999%), nitrogen (99.999%), hydrogen/argon (5 vol% H_2/Ar), ammonia/ helium (10 vol% NH_3/He) were purchased from Air Liquide. Fumed silica (Aerosil 380) was obtained from Evonik Industries. Silicalite-1 was acquired from Jincheng HuaMeiRuiZe Advanced Materials Co., Ltd. Commer- cial Beta (CP814E*, Si/Al = 12.5) and ZSM-5 (CBV 2314, Si/Al = 11.5) purchased from Zeolyst Interna- tional were calcined at 550 °C for 8 h under airflow to generate the protonated form of the zeolites.

The reference sample for UV-Vis spectrometry, $YNbO_4$, was synthesized as the procedures described by Notestein et al.[1] First, 1 g of yttrium tris(isopropoxide) and 120 mL of distilled 2-methoxyethanol were mixed in a flask and stirred for 1 h in the glovebox before attached to a Schlenk line under N_2 flow. The solution was concentrated to 3.5 mL by evaporation. Similarly, a solution of 1.2 g of niobium ethoxide and 24 mL of distilled 2-methoxyethanol was prepared and added into the yttrium solution. The mixture was concentrated to 3.5 mL, cool down to 25 °C, added to 3.5 mL of the solution of H_2O and 2-methoxyethanol (4:5 v/v), vigorously stirred for 60 s and finally poured into a watch glass. The resultant gel was dried ambiently in vacuum for 48 h, then at 300 °C in airflow to form a white solid. The product was ground with acetone and calcined at 600 °C for 12 h to yield $YNbO_4$.

2. Catalyst preparation

2.1 Preparation of mesostructured silica catalysts support

MCM-41 materials were synthesized via a post-synthesis hydrothermal method as described earlier.[2] Typically, 7.56 g of CTAB was dissolved in 52 mL distilled water in a Teflon cup under stirring. Then, 9.76 g of TEAOH (25 wt%) solution and 5 g fumed silica was added into the mixture under vigorous stirring. The mixture was stirred for 2 h at 70 °C, sealed in a Teflon-lined stainless steel autoclave, aged at 25 °C for 24 h under static conditions and treated hydrothermally for 72 h under autogenous pressure in an oven at 150 °C. The precipitated product was collected by filtration, dried at 25 °C under vacuum, ground into fine powder (grain size < 200 mesh) and transferred into a Teflon-lined stainless steel autoclave. Calculated amount of water (10 times the mass of dried product powder) was mixed with the powder. The mixture was hydrothermally treated for 24 h at 150 °C. The resultant solids were collected by filtration, washed with distilled water, vacuum dried for 12 h and calcined for 9 h at 550 °C with a heating rate of 1 °C/min under airflow. For the synthesis of MCM-41 materials with different average pore sizes, dodecyltrimethylammonium bromide or trimethyloctadecylammonium bromide was adopted as templating agent.

In a typical synthesis of HMS materials,[3] 3.08 g of dodecylamine was mixed with 83 mL ethanol + 120 mL distilled water in a Teflon cup and was stirred vigorously for 30 min, followed by the adjustment of pH to 9. Then, 17.36 g of TEOS was dropped into the solution in 40 min. The mixture was stirred for 24 h at 25 °C to form a white gel. The resultant solids were collected by filtration, washed with distilled water, dried at 100 °C for 12 h followed by calcination for 6 h at 600 °C under airflow. MCF materials were prepared similar to reported procedures:[4] First, dissolve 4.8 g of Pluronic P123 in 180 mL HCl (2 mol/L) at 40 °C under vigorous stirring for 4 h. Then, 2.4 g of TMB was added and the mixture was stirred for 4 h. Thereafter, 10.2 g of TEOS was added dropwise and was stirred for 24 h at 40 °C to form a homogeneous gel. The synthesis gel was transferred into a Teflon-lined stainless steel autoclave and treated hydrothermally for 72 h at 95 °C. The resulting solid was obtained by filtration, washed with water, dried for 12 h at 100 °C and calcined for 6 h at 550 °C under airflow. SBA-15 materials were prepared as described procedures using Pluronic P123 ($EO_{20}PO_{70}EO_{20}$) as templating agent.[5] The mass ratio of the initial solution was $EO_{20}PO_{70}$ EO_{20}:2 mol/L HCl:TEOS:H_2O = 2:60:4.25:15. After stirred for 6 h at 40 °C, the formed synthetic gel transferred to a Teflon-lined stainless steel autoclave and treated hydrothermally for 72 h at 95 °C. The solid product was recovered by filtration, washed with distilled water, dried for 12 h at 100 °C and calcined for 6 h at 550 °C under airflow. For the synthesis of KIT-6 ,[6] 2 g P123 was dissolved in a mixture of 72 g of distilled water and 3.9 g of concentrated HCl (35%). Then, 2 g of 1-butanol was added under stirring at 35 °C. After 1 h stirring, 4.3 g of TEOS was added dropwise at 35 °C, and the mixture was kept stirred for 24 h at 35 °C. The final solution transferred to a Teflon-lined stainless steel autoclave and treated hydrothermally for 72 h at 95 °C. The solid product was filtered and dried at 100 °C without washing. The template was removed by extraction in an ethanol–HCl mixture followed by calcination for 6 h at 550 °C.

2.2 Preparation of Nb-grafted MCM-41 catalysts with controlled Nb location

The Nb/MCM materials with precise control of Nb location at the internal or external surface of the MCM-41 supports were labeled Nb_{in}/MCM and Nb_{out}/MCM. For the synthesis of Nb_{in}/MCM materials, an external surface passivated method was adopted (Scheme S1). The as-synthesized MCM-41 materials were firstly pretreated with trimethoxymethylsilane. Then, the templating agent was removed by solvent extraction with $NaNO_3$ dissolved in ethanol. Thereafter, Nb species were grafted onto the surface of the passivated MCM-41 support by the VA−DI method. Finally, the grafted silanes on the external surface were removed by calcination in airflow. For the synthesis of Nb_{out}/MCM materials, the as-synthesized MCM-41 materials were directly grafted with Nb species without any treatment, and the templating agent was removed by the final step of calcination of Nb grafting procedures.

2.3 Preparation of MCM-41 supported metal oxides catalysts

The MCM-41 supported metal oxides catalysts were prepared using a similar method as the Nb-based silica catalysts in organic or aqueous media. The precursor compounds were titanium isopropoxide, vanadium tri-*i*-propoxy oxide, tantalum ethoxide or ammonium metatungstate hydrate. The titanium, vanadium, tantalum and tungstate oxide supported MCM-41 materials were denoted Ti/MCM-41, V/MCM-41, Ta/MCM-41 and W/MCM-41, respectively.

2.4 Preparation of Nb-incorporated MCM-41 catalysts

Niobium was structurally incorporated into the MCM-41-type mesoporous silica matrix (Nb-MCM) according to reported protocols by Ziolek et al.:[7] calculated amount of niobium oxalate hydrate was dissolved in 3.17 g of 0.1 mol/L oxalate acid solution (solution A). 8.08 g of sodium silicate solution was added dropwise into 50 g of distilled water under stirring and was kept stirring for 10 min (solution B). 83.75 g of CATC solution was dropped into solution B to form a homogeneous gel. Solution A was slowly added into the formed gel dropwise and was stirred for 2 h. The final pH of the synthesis gel was 11.0. The gel was transferred to a Teflon-lined stainless steel autoclave and hydrothermally treated at 100 °C for 72 h. The autoclave was cooled and unsealed every 24 h for the adjustment of pH to 11.0 by 0.1 mol/L oxalate acid solution. The solid product was filtered, washed with distilled water, dried in air for 18 h at 100 °C and calcined for 6 h at 550 °C with a heating rate of 2 °C/min in airflow to remove the templating agent.

2.5 Preparation of Nb-based MCM-41 catalysts with niobium(V) oxalate precursor

The Nb-based MCM-41 catalysts with niobium(V) oxalate precursor (Nb/MCM-ox) supported metal oxides catalysts were prepared using a similar method in aqueous media as described in ESI 2.2.

2.6 Preparation of $Nb_2O_5 \cdot nH_2O$

Hydrated amorphous niobium pentoxide ($Nb_2O_5 \cdot nH_2O$, niobic acid) was prepared as following procedures: 2 g $NbCl_5$ was mixed with 100 g of distilled water, and the mixture was stirred at 25 °C for 4 h. The resulting white precipitate was repeatedly washed with distilled water (ca. 1 L) until pH of the filtrate reached 7. Niobic acid powder was obtained by drying the precipitate overnight at 90 °C.

2.7 Preparation of Sn-Beta zeolite catalysts

The Sn-incorporated zeolites with the Beta topology were synthesized according to the reported procedures outlined by Corma et al.[8] First, 8.78 g of TEAOH (35 wt%) solution was added into 8.13 g of TEOS, followed by the addition of 0.141 g of tin chloride pentahydrate. The mixture was stirred for 16 h to ensure complete hydrolyzation of TEOS and then was partially evaporated under an IR lamp to reach the targeted H_2O/SiO_2 ratio. 1.04 g of HF was added afterwards to form a thick gel. The molar composition of the synthesis gel was 1 SiO_2/0.01 Sn/0.55 TEAOH/ 0.54 HF/7.5 H_2O. Finally, Si-Beta zeolites (5 wt% of SiO_2 in gel) were added to the mixture as seed materials. The synthesis gel was transferred to a Teflon-lined stainless steel autoclave and treated hydrothermally for 7 days at 140 °C under rotation (10 r/min). The solid product was collected by filtration, washed with distilled water, dried in air and calcined for 6 h at 550 °C with a heating rate of 2 °C/min.

The seed materials were prepared by acid-assisted dealumination of H-Beta zeolites. The parent Beta zeolite materials were treated with HNO_3 at 100 °C for 6 h under reflux conditions, then were collected by filtration, washed with distilled water and dried in air. The treatment was repeated twice to obtain Si-Beta seed materials.

2.8 Preparation of WO_x–ZrO_2 catalyst

The WO_x–ZrO_2 catalyst was synthesized via an impregnation method. Commercial $Zr(OH)_4$ was mixed with an aqueous solution of ammonium metatungstate hydrate to form a slurry, and the W loading was calculated to be 15 wt%. The result- ant was stirred by mechanical agitation for 12 h, evaporated and dried at 80 °C in air. The white solid was calcined for 6 h at 550 °C in airflow to form WO_x–ZrO_2.

3. Catalytic performance evaluation

Commercial DMF was distilled before use to remove yellow-colored impurities and a colorless purified reagent was obtained. 1,4-Dioxane was distilled to remove residual water. Prior to the reaction, the powdered catalyst was degassed for 1 h at 300 °C under dynamic vacuum (< 0.01 Pa) to remove physisorbed water. Calculated amount of catalyst, 35 mmol of DMF and 5 mL of anhydrous 1,4-dioxane, 2 mmol of naphthalene were placed into the reactor vessel, resulting a starting concentration of 4 mol/L. After the reactor was sealed, the reactor was purged three times to replace the residual air with N_2, followed by the introduction and saturation of 4 MPa ethylene. Disconnecting from ethylene gas supply, the reactor was heated to the desired temperature and started magnetic stirring with a IKA C-MAG HS 7 hot plate. For products analysis, the catalyst was separated by centrifugation and the liquid product was analyzed by gas chromatography using an Agilent 7820 GC equipped with an HP-INNO Wax capillary column (30 m × 0.25 μm × 0.32 mm) and flame ionization detector. The recycle experiments were performed with used catalysts which were collected by centrifugation, thoroughly washed with acetone under sonication for three times and finally dried at 100 °C in air before use in the next cycle.

4. Assessment of mass transfer limitations

A Weisz-Prater analysis was performed to investigate the internal mass transport resistance.[9,10]

$$C_{WP} = \frac{r_{obs}\rho_c R_p^2}{D_{eff} C_s} < 1$$

where r_{obs} ($mol \cdot kg^{-1} \cdot s^{-1}$) is the initial reaction rate, ρ_c ($kg \cdot m^{-3}$) is the bulk density of the catalyst powder, R_p (m) is the catalyst particle radius, D_{eff} ($m^2 \cdot s^{-1}$) is the effective diffusivity, C_s ($mol \cdot m^{-3}$) is the surface reactant concentration.

When C_{WP} is calculated to be <1, the internal mass transfer is negligible.

For MCM-41-based catalysts,

$r_{obs} = 0.02069$ ($mol \cdot kg^{-1} \cdot s^{-1}$)

$\rho_c = 3\times10^2$ ($kg \cdot m^{-3}$)

$R_p = 6.25\times10^{-5}$ (m) (120 mesh particles)

$C_s = 3.13\times10^3$ ($mol \cdot m^{-3}$) (Calculated from adsorption experiments, see Table S6)

For the calculation of D_{eff},

$$D_{eff} = \frac{\varepsilon D_{AB}}{\tau}$$

The bulk diffusivity D_{AB} can be estimated by the Fuller correlation:[10]

$$D_{AB} = \frac{1.00\times10^{-7} T^{1.75} \left(\frac{1}{M_A} + \frac{1}{M_B}\right)^{0.5}}{p\left[(\sum_i v_{iA})^{\frac{1}{3}} + (\sum_i v_{iB})^{\frac{1}{3}}\right]^2}$$

where T (K) is the temperature, M_A, M_B (g/mol) are molecular weights of A and B, p (atm) is pressure, $v_{i,j}$ are the volumes of parts of the molecule j.

The tortuosity τ was calculated from the Bruggeman relation:[10]

$$\tau = \varepsilon^{-0.5} = (1 - \frac{\rho_b}{\rho_p})^{-0.5}$$

where ρ_b, ρ_p are the bulk density of the porous catalyst and the intrinsic density of the catalyst material.

To estimate the diffusivity D_{AB} for 2,5-DMF (A, C_6H_8O) in 1,4-dioxane (B, $C_4H_8O_2$) under reaction conditions, the kinetic parameters are listed below:

M_{DMF} = 96.13 g/mol, $M_{dioxane}$ = 88.11 g/mol, v_C = 15.9, v_H = 2.31, v_O = 6.11, p = 1 atm (for liquid phase), T = 523 K.

Afterwards, the value of D_{AB} was to be determined as follows:

$$D_{AB} = \frac{1.00\times10^{-7}\times573^{1.75}\times\left(\frac{1}{96.13} + \frac{1}{88.11}\right)^{0.5}}{1\times\left[(15.9\times6 + 2.31\times8 + 6.11\times1)^{\frac{1}{3}} + (15.9\times4 + 2.31\times8 + 6.11\times2)^{\frac{1}{3}}\right]^2}$$

$$D_{AB} = 1.10\times10^{-5}(m^2/s)$$

Therefore, the effective diffusivity in MCM-41 materials were:

$$D_{eff} = \frac{\varepsilon D_{AB}}{\tau} = (1 - \frac{\rho_b}{\rho_p})^{1.5}\times D_{AB}$$

$$D_{eff} = 0.42^{1.5}\times1.10\times10^{-5} = 2.99\times10^{-6}(m^2/s)$$

Finally, the value of C_{WP} was determined to be:

$$C_{WP} = \frac{r_{obs}\rho_c R_p^2}{D_{eff}C_s} = \frac{0.02069\times3\times10^2\times(6.25\times10^{-5})^2}{2.99\times10^{-6}\times3.13\times10^3} = 2.59\times10^{-6} \ll 1$$

The absence of internal mass transfer limitations with the MCM-41-based catalytic system was verified.

The elimination of external mass transfer limitations was confirmed by investigating the influence of the magnetic stirring speed on the initial reaction rate in 0.5 h.[11] In the stirring speed range of 500−1200 r/min under reaction conditions, the initial reaction rate kept unchanged, which proved the absence of external mass transfer limitations within the catalytic system.

5. Kinetic simulation of liquid-phase adsorption

The adsorption of DMF on siliceous supports was simulated with the pseudo-second-order kinetic model, assuming the reversible equilibrium between the solid and the adsorbate in liquid phase.[12] The values of rate constant k_2 and equilibrated adsorption amount Q_e were calculated from as follows:[13]

$$Q_t \text{ (mmol/g)} = \frac{Q_e^2 k t}{1+Q_e k t}$$

where k (g·min^{-1}·mmol^{-1}), Q_e (mmol/g), Q_t (mmol/g) and t (min) are the sorption rate constant for pseudo-second-order kinetic model, the equilibrated adsorption amount, the amount of adsorbate per unit mass of the adsorbent, and contact time, respectively.

The concentration of adsorbate in the channels/pores of adsorbate C_{in} and the concentration in the liquid phase C_{out} and the ratio C_{in}/C_{out} were calculated as follows:

$$C_{in}/C_{out} = \frac{Q_e/V_{total}}{C_{liq.}}$$

where Q_e (mmol/g), V_{total} (mL/g) and $C_{liq.}$(mmol/mL) are the equilibrated adsorption amount, the total pore volume obtained from N_2 sorption experiments, the concentration of the adsorbate in the liquid phase at equilibrium.

6. Model reactions

6.1 Cycloaddition of maleic anhydride with 2,3-dimethyl-1,3-butadiene

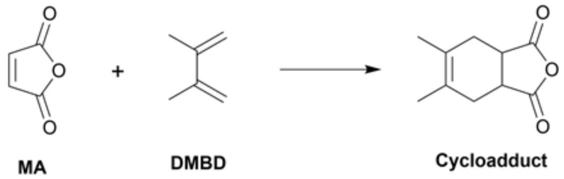

Maleic anhydride (MA, 2 mmol, 0.196 g), 2,3-dimethyl-1,3-butadiene (DMBD, 3 mmol, 0.246 g), solvent (10 mL) and catalyst (100 mg) were added into a 50 mL sealed flask. The mixture was stirred under N_2 atmosphere at 60 °C for 1 h. The catalyst was separated by centrifugation and the purified product was further identified by ^1H and ^{13}C NMR (Fig. S22)

6.2 Dehydration of cyclohexanol

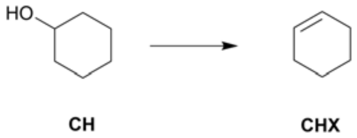

Cyclohexanol (CH, 4 mmol, 0.401 g), solvent (10 mL) and catalyst (100 mg) were added into a 50 mL sealed tube under N_2 flow. Subsequently, the mixture was stirred at 80 °C for 2 h. After separation of catalyst, the product was purified and identified by ^1H and ^{13}C NMR (Fig. S23).

7. Supplementary data

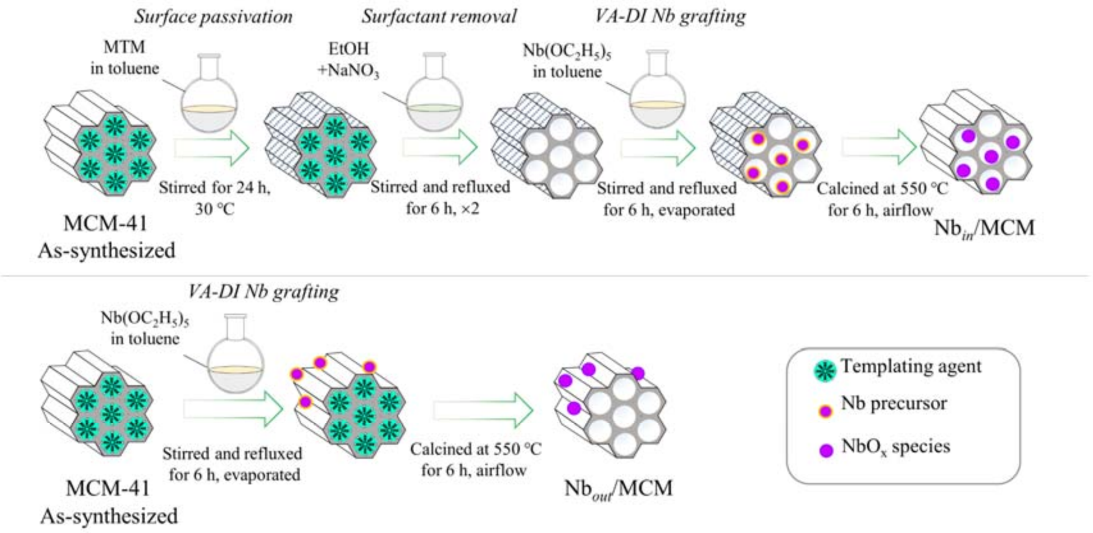

Scheme S1. Preparation of 2Nb*in*/MCM and 2Nb*out*/MCM catalysts.

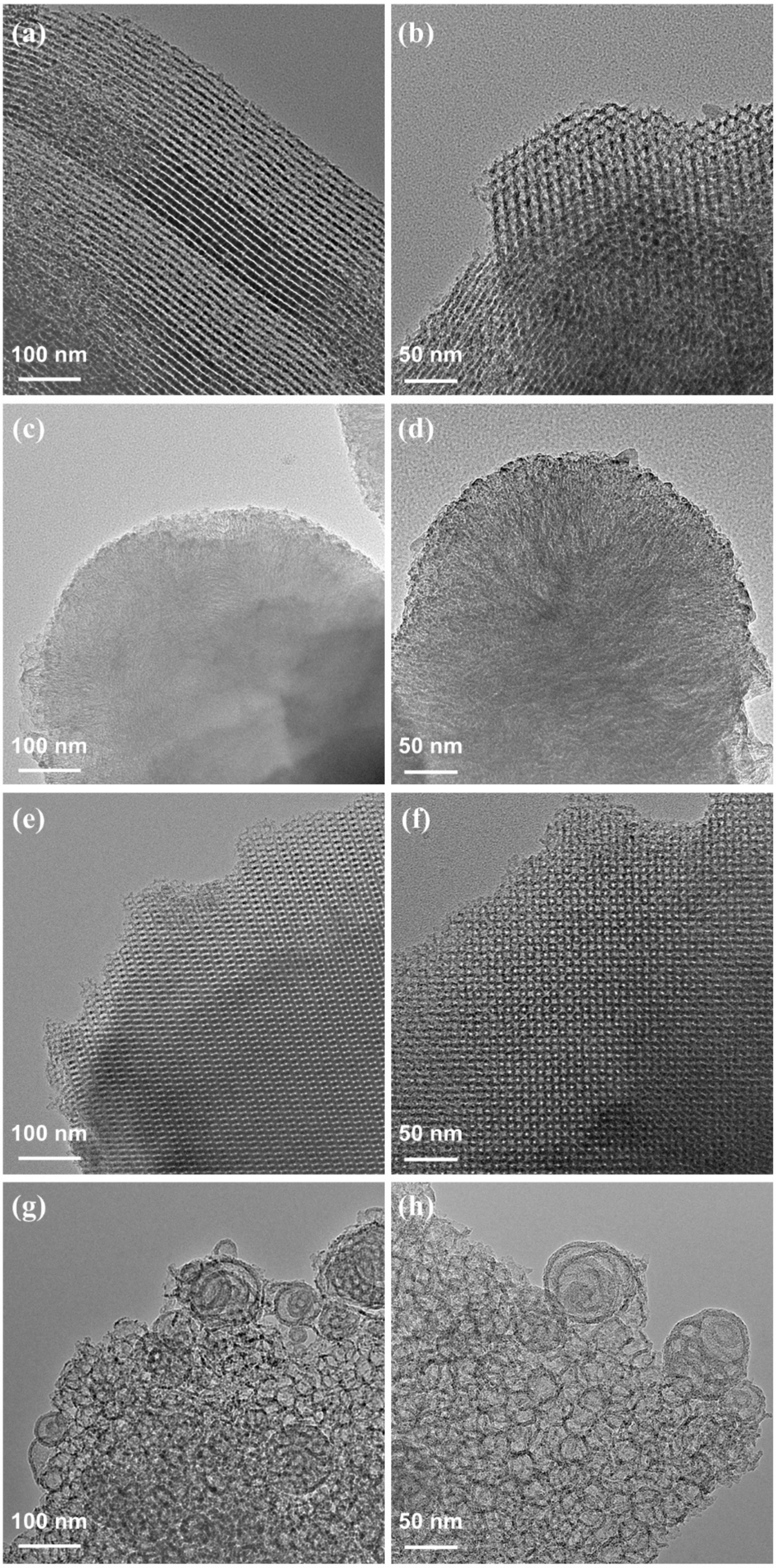
(a)
100 nm
(b)
50 nm
(c)
100 nm
(d)
50 nm
(e)
100 nm
(f)
50 nm
(g)
100 nm
(h)
50 nm

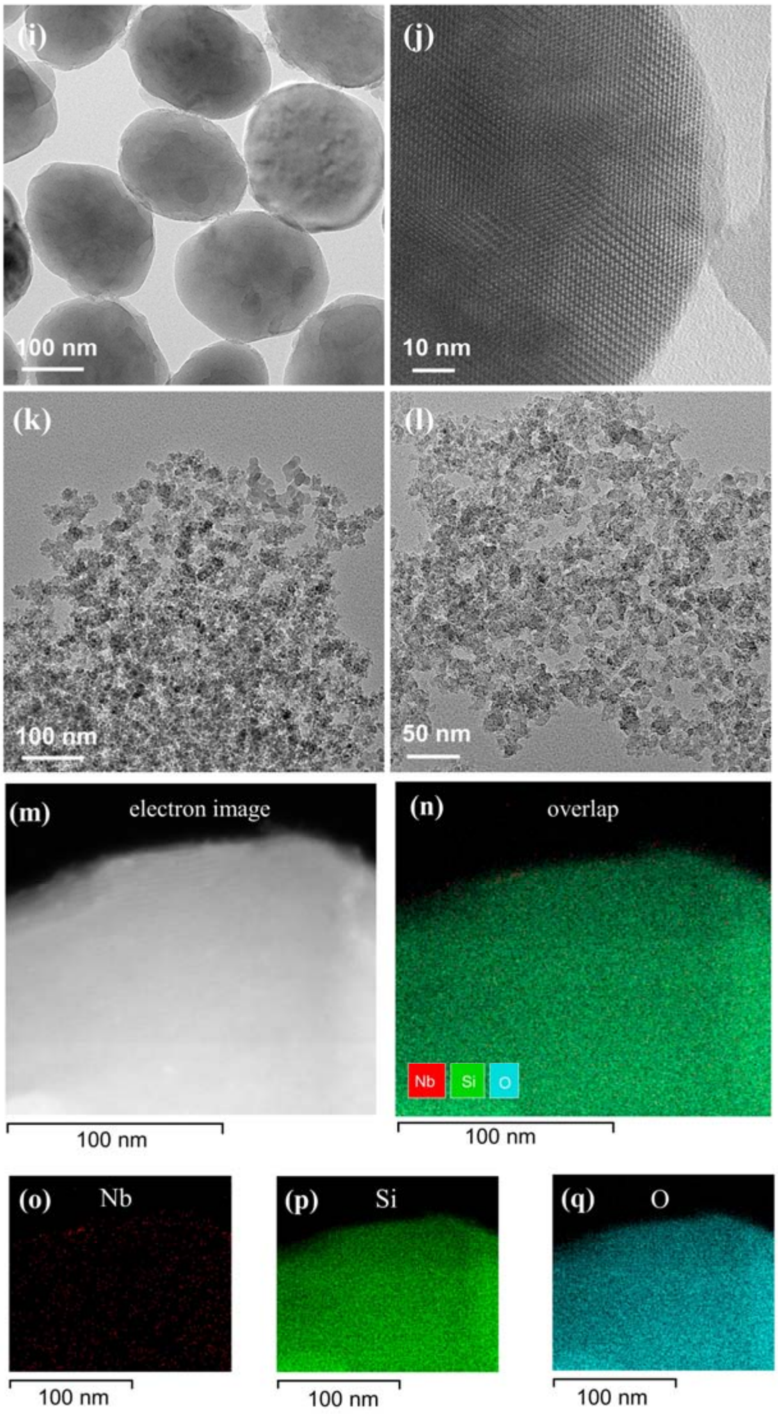

Fig. S1. HRTEM images of 2 wt% Nb-based SBA-15 (a, b), HMS (c, d), KIT-6 (e, f), MCF (g, h), S-1 (i, j), SiO_2 (k, l) catalysts and EDX mapping images (m−q) for 2 wt% Nb/MCM catalyst.

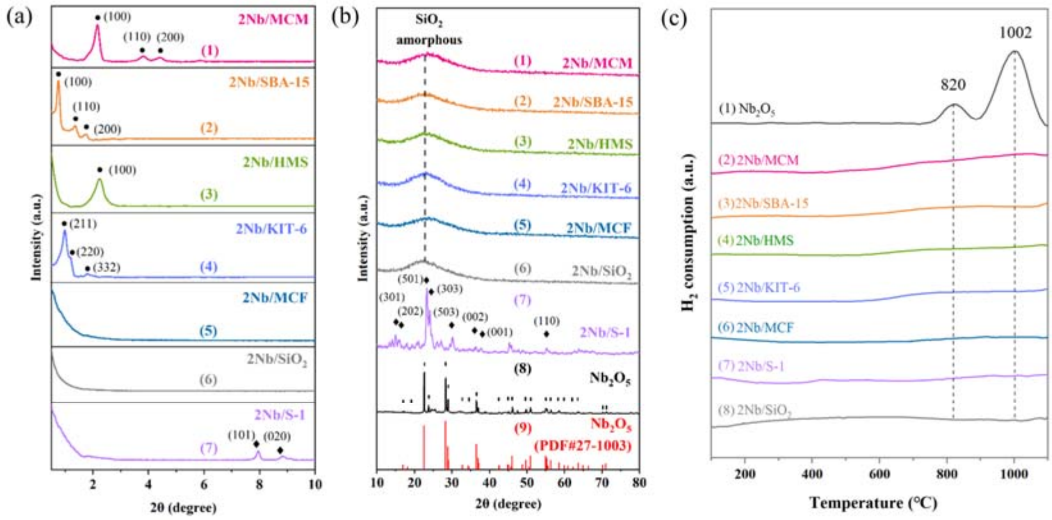

Fig. S2. Small-angle (a), wide-angle (b) XRD patterns and H_2−TPR profiles (c) of 2 wt% Nb-based silica catalysts.

Table S1. Physicochemical properties of the Nb-based silica materials.

Entry	Sample	Nb loading [a] (wt%)	S_{total} [b] (m^2/g)	d_p [c] (nm)	V_{total} [b] (cm^3/g)
1	2Nb/MCM	1.86	824	3.5	0.89
2	2Nb/SBA-15	1.93	552	8.4	1.18
3	2Nb/HMS	1.87	993	2.9	0.82
4	2Nb/KIT-6	1.91	515	5.7	0.68
5	2Nb/MCF	1.88	616	14.1	1.74
6	2Nb/S-1	1.78	368	0.57	0.17
7	2Nb/SiO_2	1.95	341	15.8	0.50
8	2Nb/silica gel	1.97	328	22.3	0.42

[a] Determined by ICP−AES. [b] S_{total}, V_{total} were the total surface area and pore volume which were obtained by BET method. [c] d_p was the average pore diameter calculated from the desorption isotherm from BJH method.

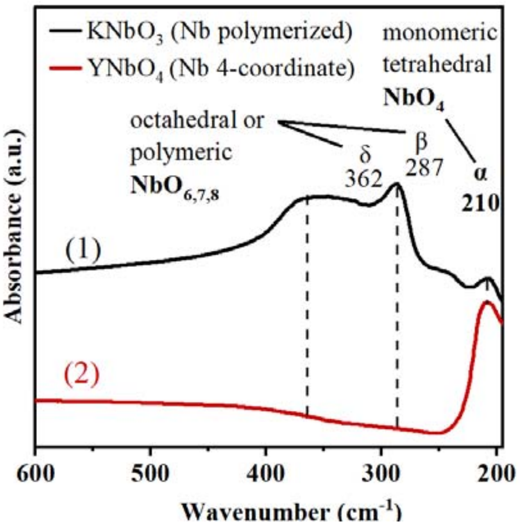

Fig. S3. UV−Vis spectra of reference samples. (1) $KNbO_3$, (2) $YNbO_4$.

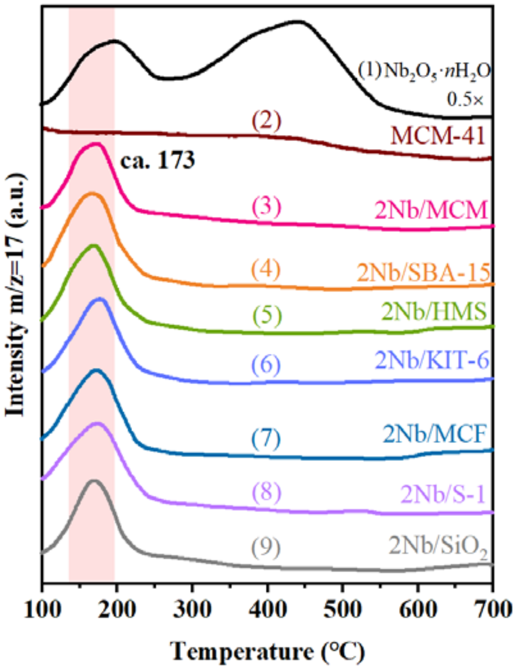

Fig. S4. NH_3–TPD–MS profiles of the Nb-based catalyst samples. (1) $Nb_2O_5\cdot nH_2O$, (2) MCM-41, (3) 2Nb/MCM, (4) 2Nb/SBA-15, (5) 2Nb/HMS, (6) 2Nb/KIT-6, (7) 2Nb/MCF, (8) 2Nb/S-1, (9) 2Nb/SiO_2

Table S2. Acidic properties of the Nb-based silica materials.

Entry	Sample	Total acidity [a] (mmol/g)	Py acid density [b] (mmol/g)	
			L acid	B acid
1	2Nb/MCM	0.118	0.074	N.A.
2	2Nb/SBA-15	0.121	0.080	N.A.
3	2Nb/HMS	0.115	0.081	N.A.
4	2Nb/KIT-6	0.119	0.077	N.A.
5	2Nb/MCF	0.125	0.072	N.A.
6	2Nb/S-1	0.122	0.068	N.A.
7	2Nb/SiO_2	0.109	0.078	N.A.
8	$Nb_2O_5\cdot nH_2O$	1.642	0.603	0.766
9	MCM-41	N.A.	N.A.	N.A.

[a] Quantified based on calibrated integrated areas of the desorption peak in NH_3–TPD–MS experiments.

[b] Determined by FT-IR spectra of adsorbed pyridine at 150 °C.

Table S3. Catalytic conversion of DMF and ethylene into PX over Nb-free silicas.

Entry	Catalyst	DMF Conv.	Selectivity (%)				CB
		(%)	PX	DMCHO	MPB	HDO	(%)
1	SBA-15	<1	-	-	-	-	>99
2	HMS	<1	-	-	-	-	>99
3	KIT-6	<1	-	-	-	-	>99
4	MCF	<1	-	-	-	-	>99
5	S-1	<1	-	-	-	-	>99
6	SiO_2	<1	-	-	-	-	>99
7	silica gel	<1	-	-	-	-	>99

Reaction conditions: DMF (35 mmol), C2H4 (4 MPa), 1,4-dioxane (5 mL), catalyst (0.12 g), 250 °C, 2 h.

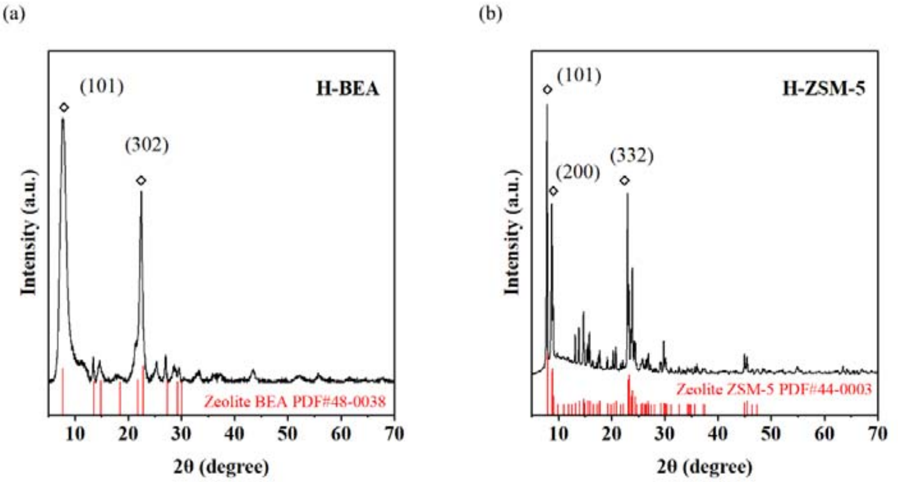

Fig. S5. XRD patterns of H-Beta (a) and H-ZSM-5 (b) catalyst samples.

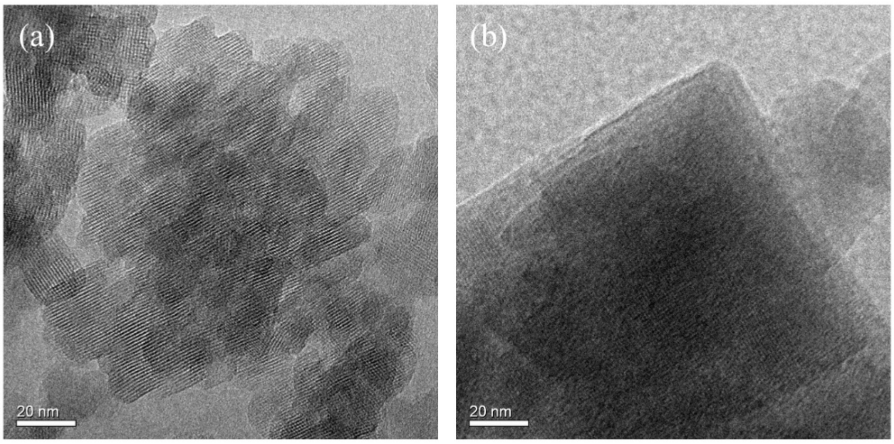

Fig. S6. HRTEM images of H-BEA (a) and H-ZSM-5 (b) catalyst samples.

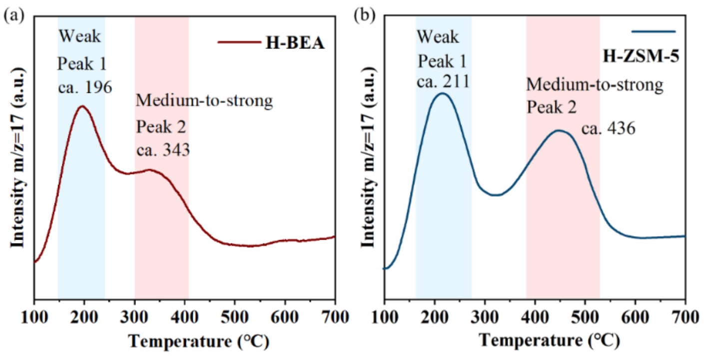

Fig. S7. NH_3–TPD–MS profiles of H-BEA (a) and H-ZSM-5 (b) catalyst samples.

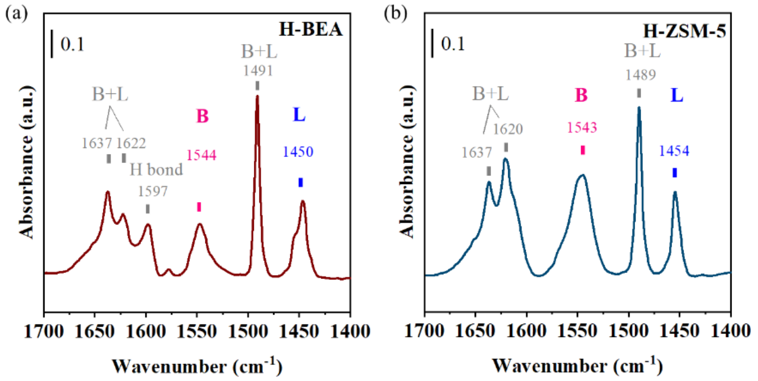

Fig. S8. Pyridine adsorbed FTIR spectra of H-BEA (a) and H-ZSM-5 (b) samples.

Table S4. Physicochemical properties of H-BEA and H-ZSM-5 catalyst samples.

Entry	Sample	SAR [a]	Surface area (m^2/g)			V_{total} [e] (cm^3/g)	Total acidity [f] (mmol/g)	Py acidity [g] (μmol/g)	
			S_{total} [b]	S_{micro} [c]	$S_{ext.}$ [d]			L	B
1	H-BEA	14.1	582	339	243	0.85	1.106	383	296
2	H-ZSM-5	12.7	413	297	116	0.24	1.335	219	562

[a] SAR represents Si/Al ratio determined by ICP–AES. [b] S_{total} was the total surface area obtained by Brunauer–Emmett–Teller method. [c] S_{micro} was the surface area of micropores calculated from *t*-plot. [d] $S_{ext.} = S_{total} - S_{micro}$. [e] Vtotal was the total pore volume obtained by BET method. [f] Total acidity was quantified based on calibrated integrated areas of the desorption peak in NH_3–TPD–MS experiments. g Determined by FT-IR spectra of adsorbed pyridine at 150 °C.

Table S5. Catalytic conversion of DMF and ethylene into PX over MCM-41 supported catalysts.

Entry	Catalyst	DMF Conv. (%)	Selectivity (%)				CB (%)	PX Yield (%)
			PX	DMCHO	MPB	HDO		
1	2Ti/MCM-41	29	90	5	3	2	98	24
2	2V/MCM-41	32	91	3	2	4	87	17
3	2Ta/MCM-41	41	91	4	3	2	96	34
4	2W/MCM-41	40	88	4	3	5	89	26
5	2Al/MCM-41	35	89	5	3	3	90	22

Reaction conditions: DMF (35 mmol), C_2H_4 (4 MPa), 1,4-dioxane (5 mL), catalyst (0.12 g), 250 °C, 2 h.

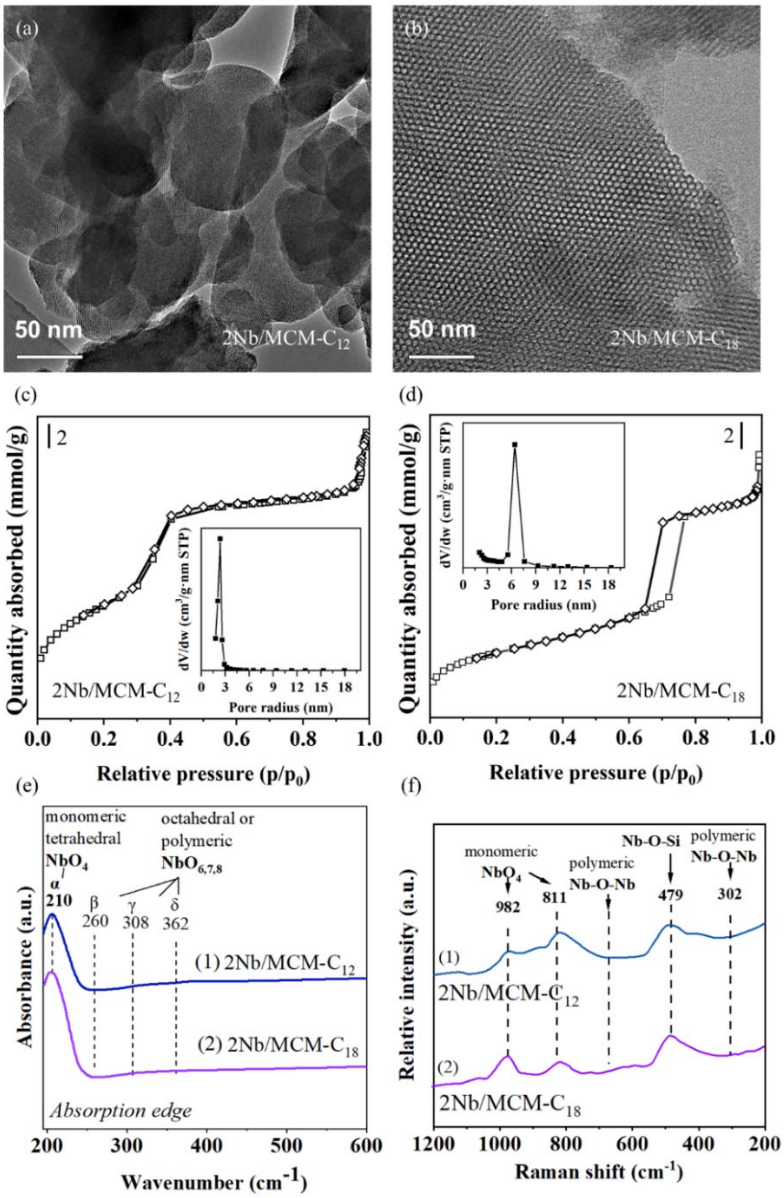

Fig. S9. HRTEM images (a, b), N_2 sorption isotherms and pore size distribution (c, d), UV−Vis spectra (e) and Raman spectra (f) of 2Nb/MCM materials prepared with various surfactants.

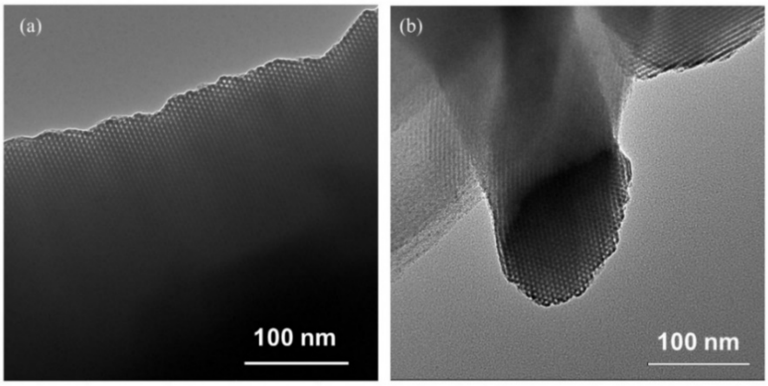

Fig. S10. HRTEM images of $2Nb_{in}$/MCM (a) and $2Nb_{out}$/MCM (b) samples.

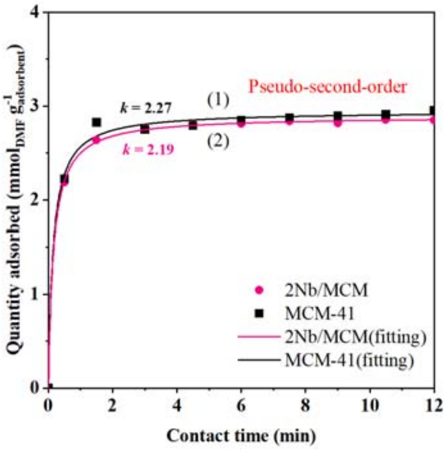

Fig. S11. Adsorption kinetics of DMF onto MCM-41 support (1) and 2Nb/MCM (2) in 1,4-dioxane at 30 °C.

Table S6. Kinetic parameters for adsorption on siliceous catalyst supports at 30 °C.

Entry	Adsorbent	k [a] (g·min^{-1} ·mmol^{-1})	Q_e [a] (mmol/g)	R^2 [a]	V_{total} [b] (cm^3/g)	C_s [c] (M)	C_{in}/C_{out}
1	MCM-41	2.27	2.94	0.995	0.94	3.13	16.0
2	SBA-15	1.73	2.68	0.999	1.21	2.21	11.4
3	HMS	1.70	2.61	0.999	0.92	2.84	14.5
4	KIT-6	1.53	2.28	0.993	0.73	3.12	15.8
5	MCF	-	1.98	-	1.81	1.10	-
6	S-1	-	1.27	-	0.21	6.04	-
7	SiO_2	-	0.40	-	0.52	0.77	-
8	2Nb/MCM	2.19	2.86	0.999	0.89	3.21	16.5

[a] k (g·min^{-1}·mmol^{-1}), Q_e (mmol/g) were sorption rate constant and equilibrated adsorption amount calculated from pseudo-second-order kinetic model. R^2 was the coefficient of determination for curve fitting. The Q_e values of MCF, S-1, SiO_2 were the quantity adsorbed at equilibrium (contact time = 12 min). [b] V_{total} was the total pore volume obtained by BET method. [c] C_s was the normalized specific quantity adsorbed based on V_{total}. For the pseudo-second-order-type adsorption, $C_s = C_{in}$.

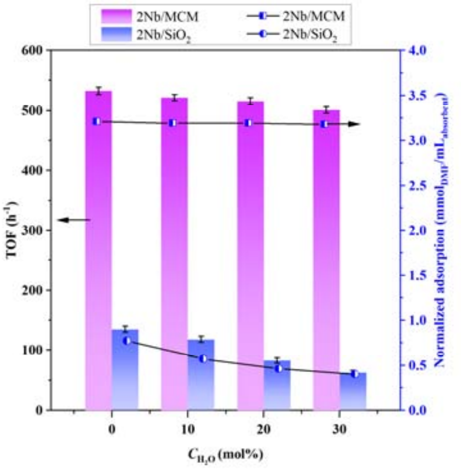

Fig. S12. Initial reaction rate for PX synthesis and DMF adsorption at equilibrium under 30 °C with various concentration of water. Reaction conditions: DMF (35 mmol), C_2H_4 (4 MPa), 1,4-dioxane (5 mL), catalyst (0.12 g), 250 °C.

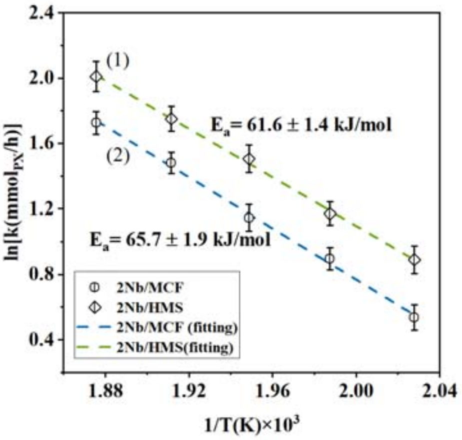

Fig. S13. Arrhenius plot in the range of 220−260 °C for 2Nb/HMS (1) and 2Nb/MCF (2) catalysts. Reaction conditions: DMF (35 mmol), C_2H_4 (4 MPa), 1,4-dioxane (5 mL), catalyst (0.12 g).

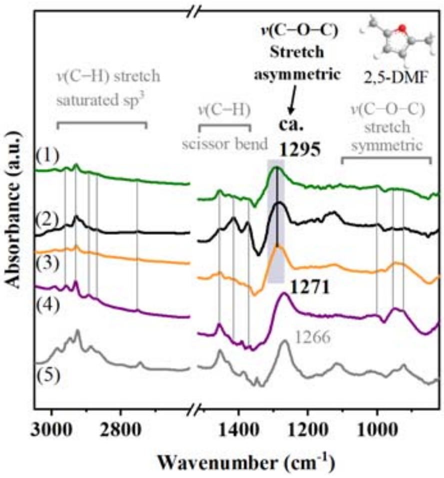

Fig. S14. DRIFT spectra of 2,5-DMF adsorption on Nb-based catalysts at 90 °C. (1) 2Nb/MCM, (2) 2Nb/MCM-C_{18}, (3) 2Nb/SiO_2, (4) MCM-41, (5) neat DMF.

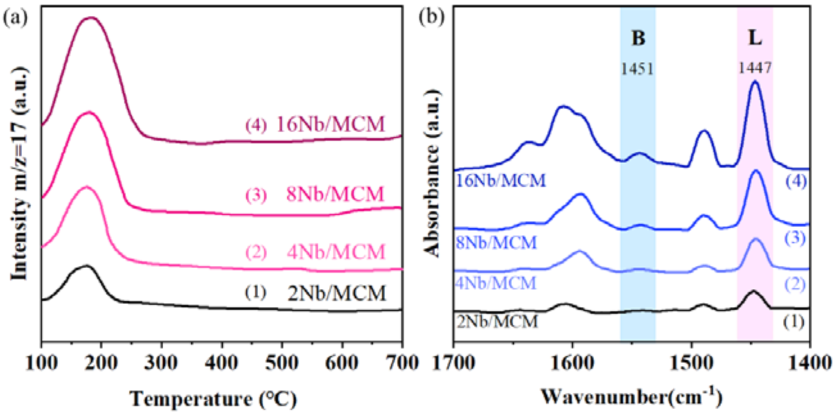

Fig. S15. NH_3–TPD–MS profiles (a) and pyridine adsorbed FTIR spectra (b) of Nb/MCM based catalyst samples. (1) 2Nb/MCM, (2) 4Nb/MCM, (3) 8Nb/MCM, (4) 16Nb/MCM.

Table S7. Acidic properties of Nb -based MCM-type catalysts.

Entry	Sample	SNR [a]	Total acidity [b] (mmol/g)	Py acidity [c] (mmol/g)		B/L
				L	B	
1	8Nb/MCM-*ox*	8.13	0.448	0.353	0.042	0.12
2	8Nb-MCM	7.51	0.349	0.247	0.085	0.34

[a] SNR represents Si/Nb ratio determined by ICP–AES. [b] Total acidity was quantified based on calibrated integrated areas of the desorption peak in NH_3–TPD–MS experiments. [c] Determined by FT-IR spectra of adsorbed pyridine at 150 °C.

Table S8. Catalytic conversion of DMF and ethylene into PX over Nb -based MCM-type catalysts.

Entry	Catalyst	DMF Conv. (%)	Selectivity (%)				CB (%)	PX Yield (%)
			PX	DMCHO	MPB	HDO		
1	8Nb/MCM-*ox*	53	93	1	2	4	92	42
2	8Nb-MCM	57	87	2	5	6	82	34

Reaction conditions: DMF (35 mmol), C_2H_4 (4 MPa), 1,4-dioxane (5 mL), catalyst (0.033 g), 250 °C, 2 h.

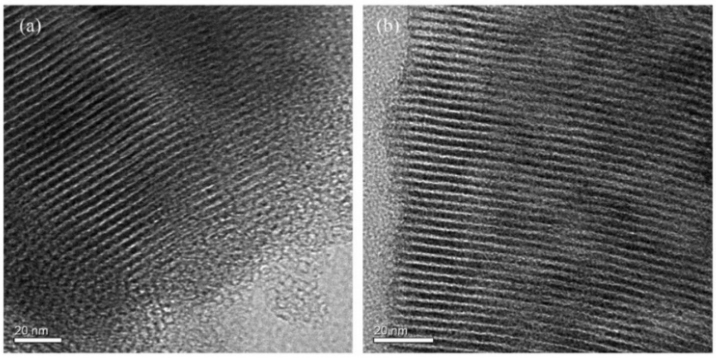

Fig. S16. HRTEM images of Nb-based MCM-41 materials. (a) 8Nb-MCM prepared by a hydrothermal method, (b) 8Nb/MCM-*ox* synthesized from niobium oxalate precursor.

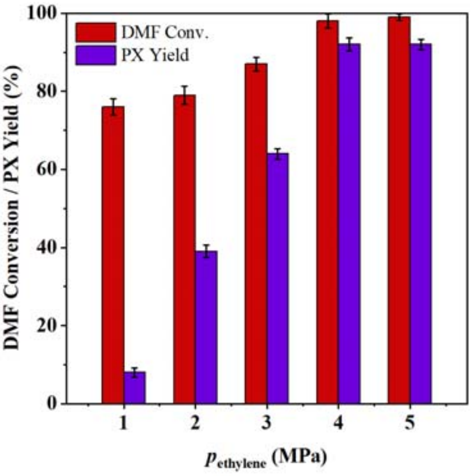

Fig. S17. Influence of ethylene pressure on the catalytic performance of 8Nb/MCM catalysts for PX synthesis. Reaction conditions: DMF (35 mmol), C_2H_4 (1−5 MPa), 1,4-dioxane (5 mL), catalyst (0.033 g), 250 °C, 6 h.

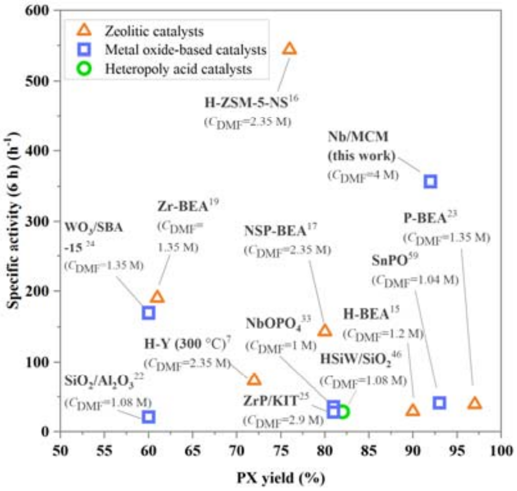

Fig. S18. Performance comparison of Nb/MCM catalyst with other reported catalytic systems for PX synthesis from DMF and ethylene at 250 °C. The specific activity value were calculated based on 6 h reaction. The PX yield was maximum value for the catalytic system.

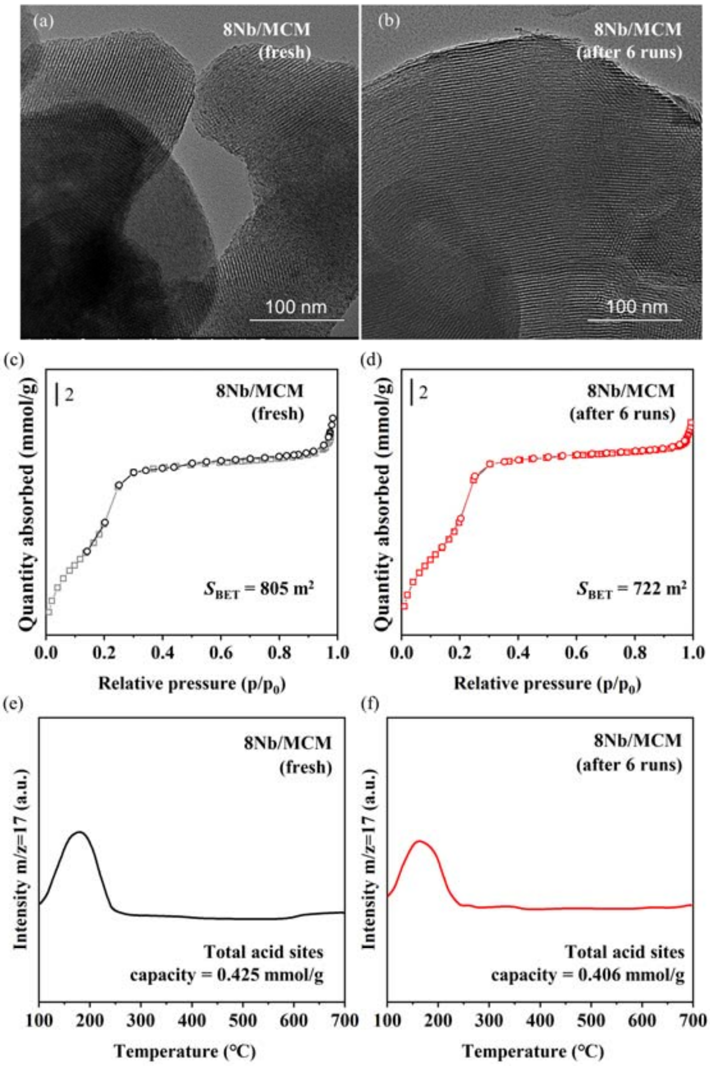

Fig. S19. HRTEM images (a, b), N_2 sorption isotherms and pore size distribution (c, d), NH_3−TPD−MS profiles (e, f) of 8Nb/MCM catalyst before and after use.

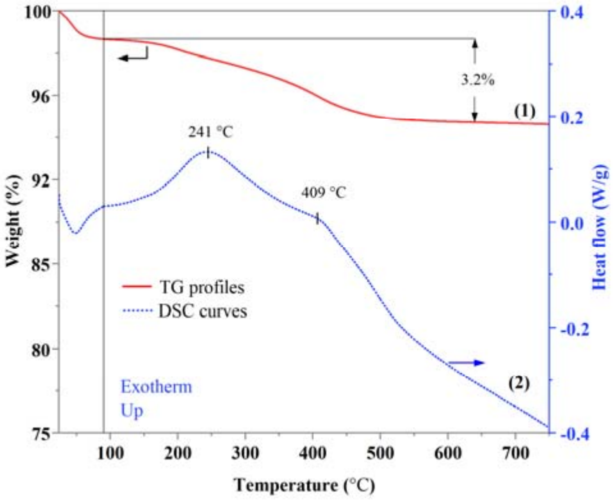

Fig. S20. TG-DSC profiles of the spent 8Nb/MCM catalysts after six successive runs.

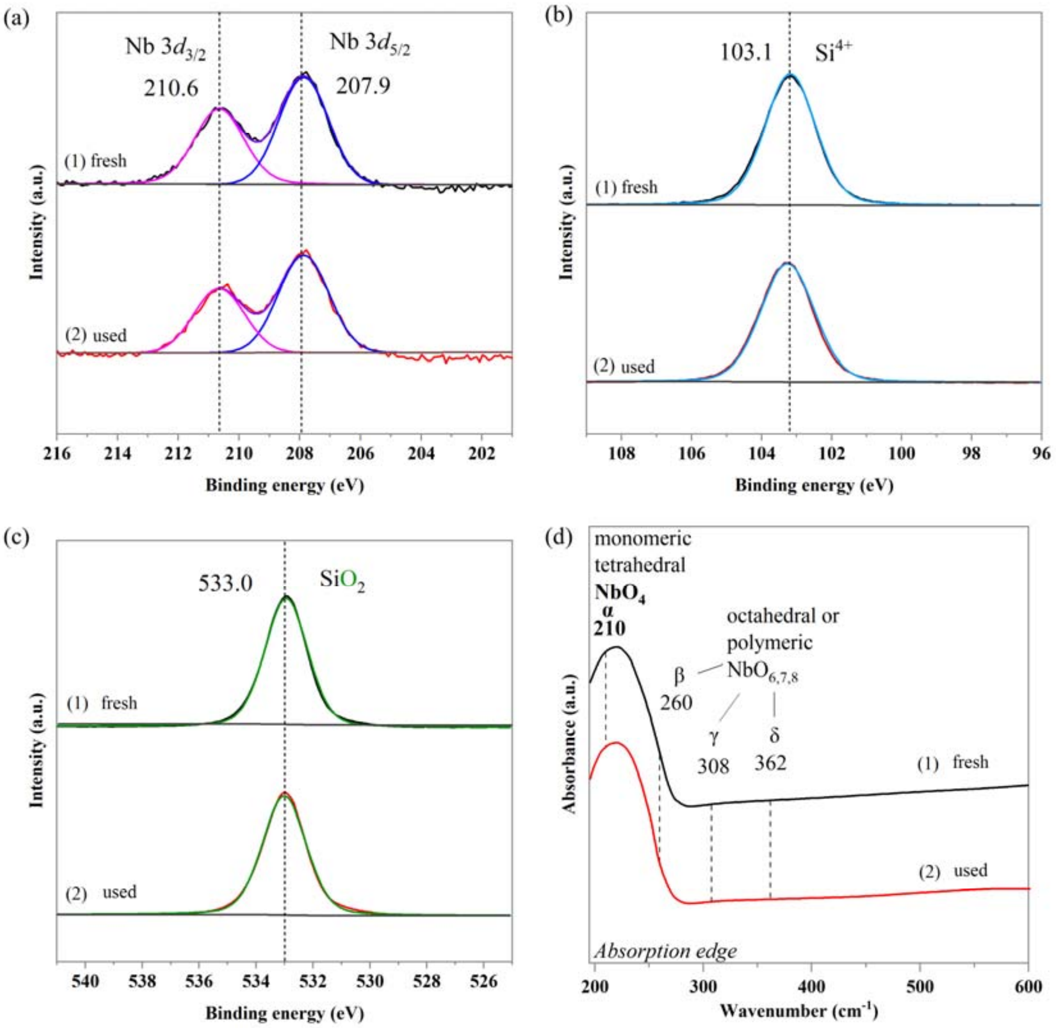

Fig. S21. Comparison of the fresh and used 8Nb/MCM catalyst after six successive runs. XPS spectra the regions for Nb $3d_{5/2}$ and Nb $3d_{3/2}$ (a), Si 2*p* (b) and O 1*s* (c) and UV−Vis spectra (d).

Table S9. The PX-mediated process for DMF and ethylene conversion over 8Nb/MCM catalyst.

Entry	C_{DMF} [a] (mol/L)	DMF Conv. (%)	Selectivity (%)				CB (%)	PX Yield (%)
			PX	DMCHO	MPB	HDO		
1 [b]	4	>99	95	1	3	1	94	89
2 [c]	6	>99	87	3	6	4	91	79

Reaction conditions: C_2H_4 (4 MPa), PX (5 mL), catalyst (0.033 g), 250 °C.

[a] C_{DMF} was the initial concentration of DMF in the catalytic system. [b] 10 h. [c] 12 h.

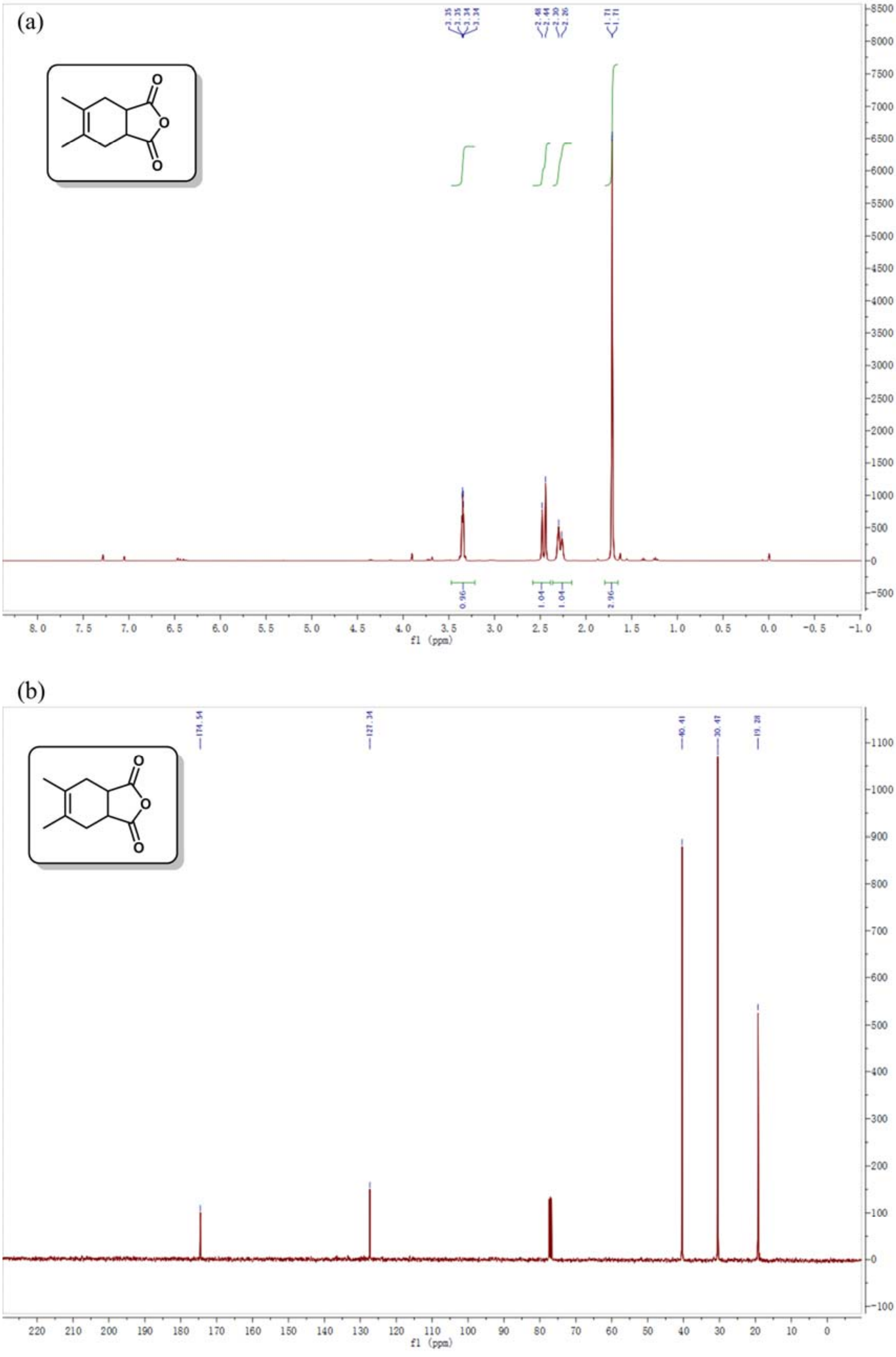

Fig. S22. ^{1}H-NMR (a) and ^{13}C-NMR (b) data for the cycloadduct of maleic anhydride with 2,3-dimethyl-1,3-butadiene.

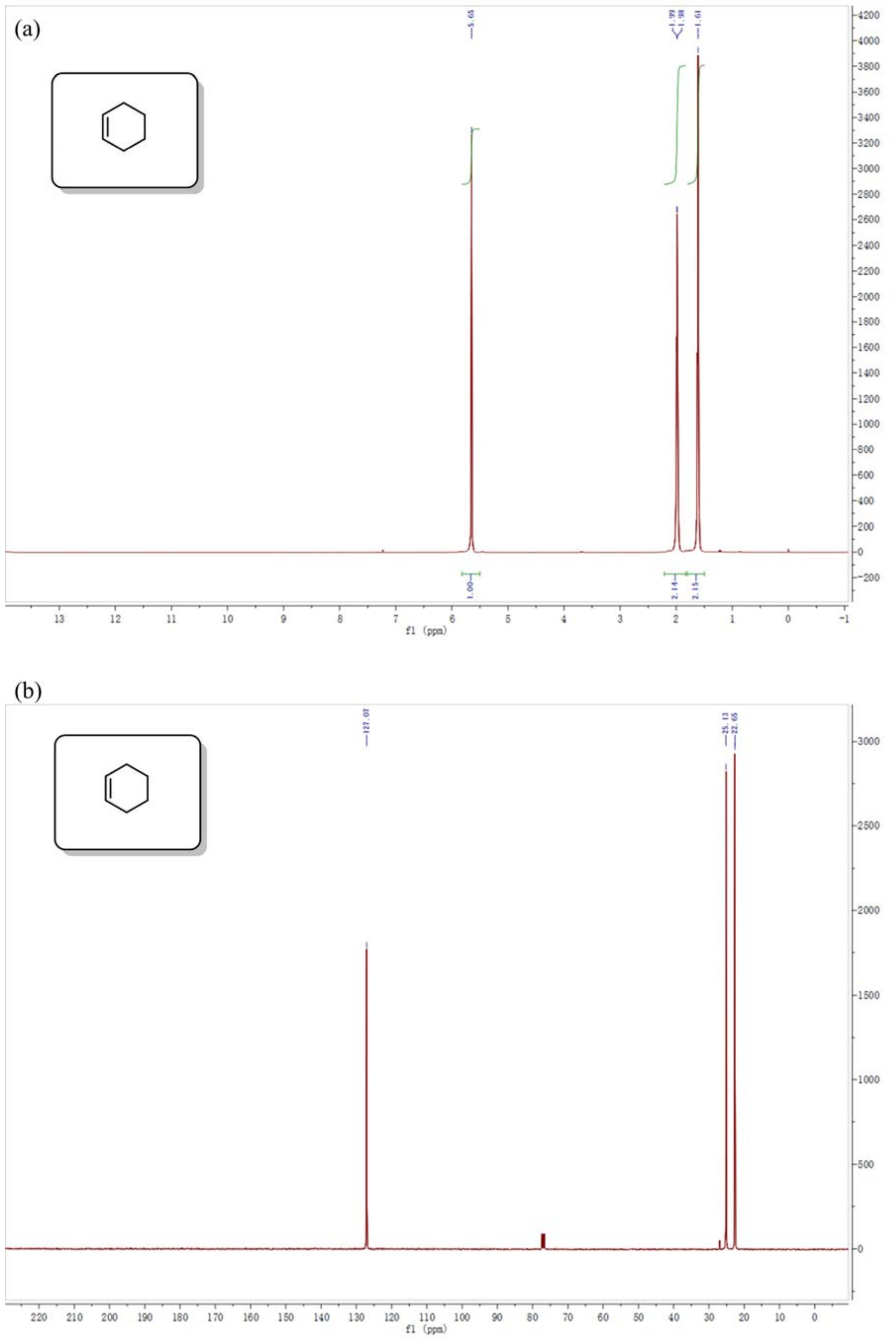

Fig. S23. ^{1}H-NMR (a) and ^{13}C-NMR (b) data for the product of cyclohexanol dehydration.

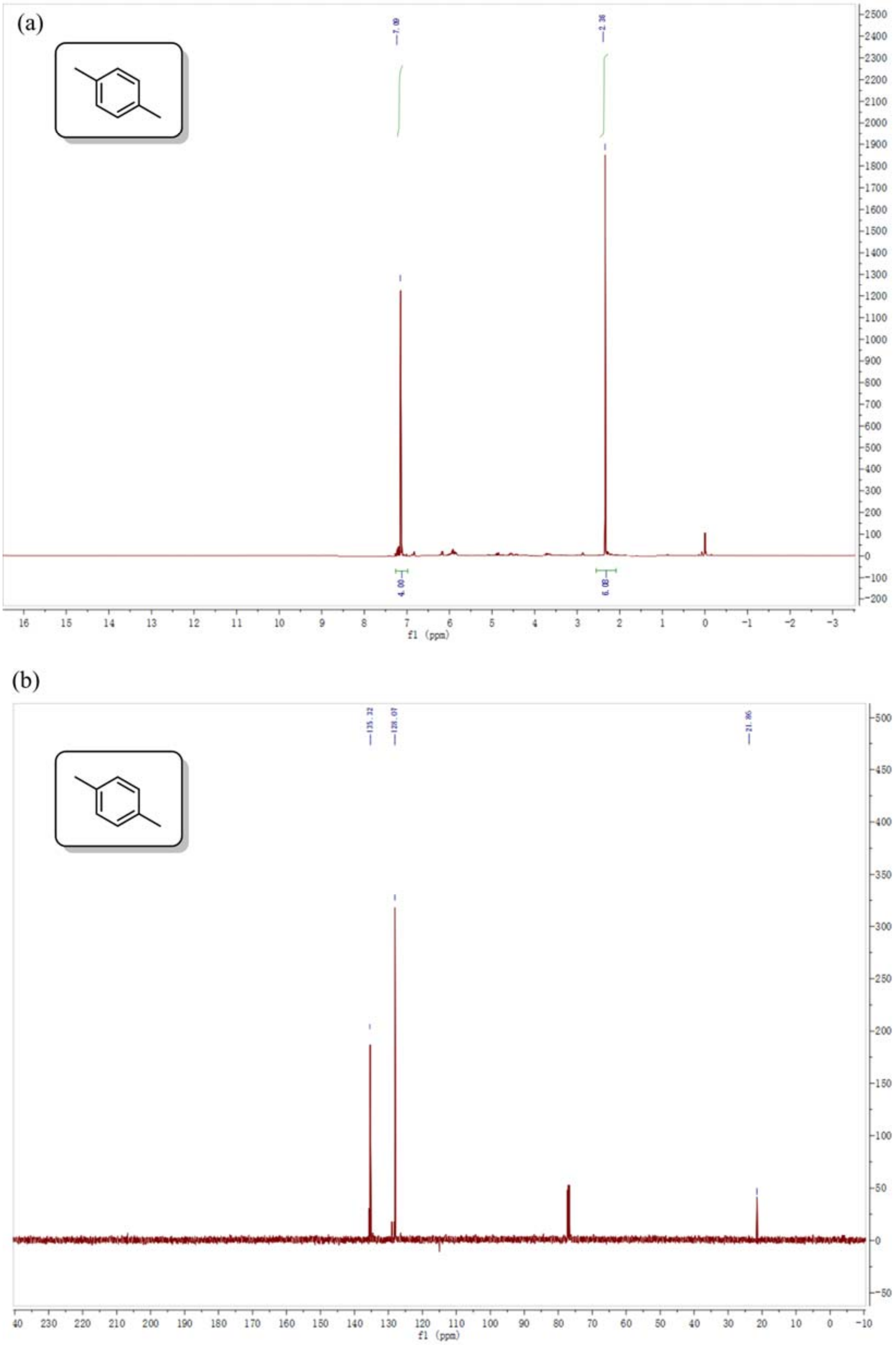

Fig. S24. ^{1}H-NMR (a) and ^{13}C-NMR (b) data for the isolated PX.

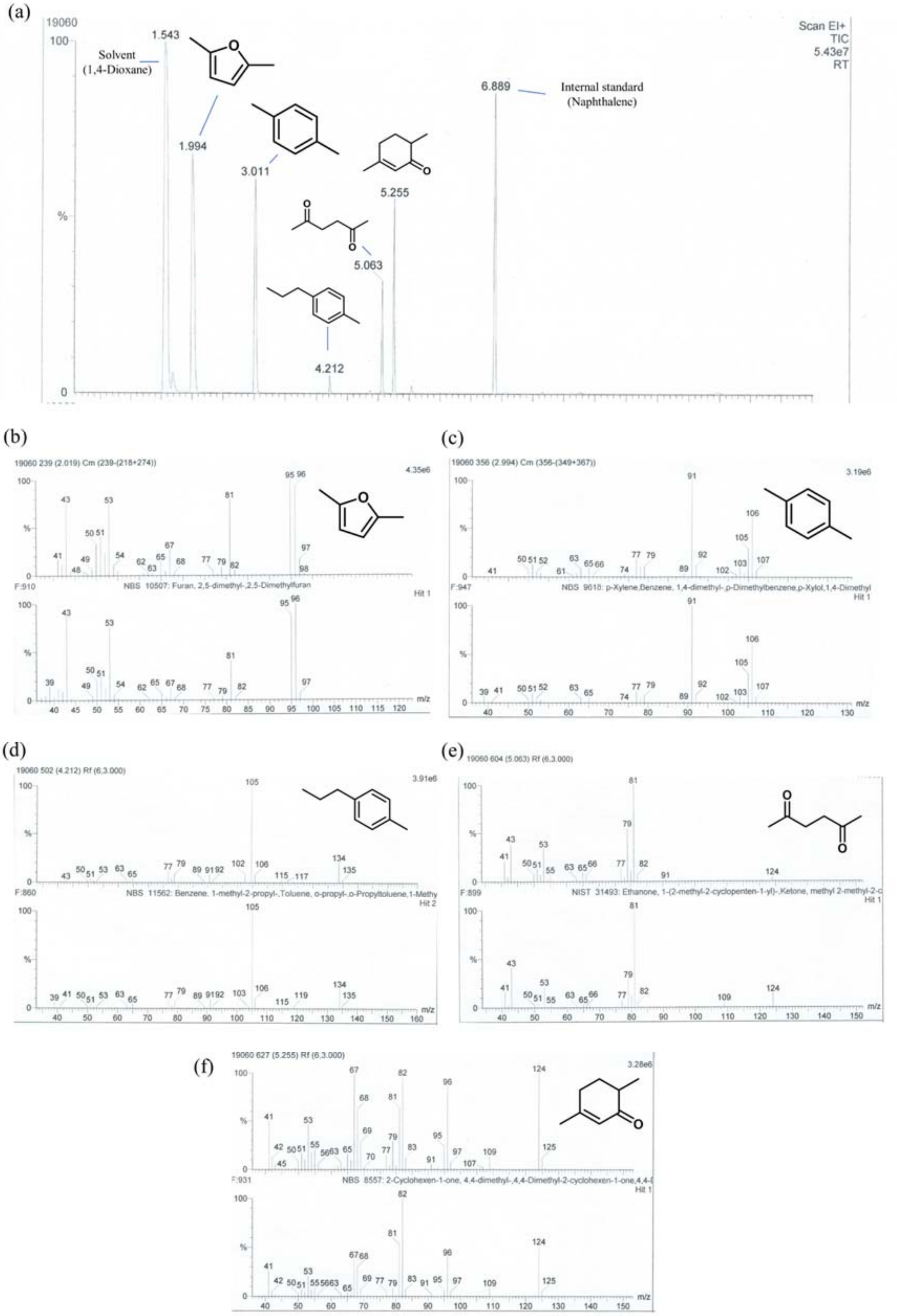

Fig. S25. GC-MS data copy for the DMF-to-PX process. (a) GC chromatograms. The mass spectra acquired for DMF (a), PX (b), MPB (c), HDO (d), DMCHO (e).

Notes and references

[1] N. E. Thornburg, A. B. Thompson, J. M. Notestein, *ACS Catal.*, 2015, **5**, 5077–5088.

[2] L. Chen, T. Horiuchi, T. Mori, K. Maeda, *J. Phys. Chem. B*, 1999, **103**, 1216–1222.

[3] T. R. Pauly, Y. Liu, T. J. Pinnavaia, S. J. L. Billinge, T. P. Rieker, *J. Am. Chem. Soc.*, 1999, **121**, 8835–8842.

[4] Y. M. Liu, J. Xu, L. C. Wang, Y. Cao, H. Y. He, K. N. Fan, *Catal. Lett*., 2008, **125**, 62–68.

[5] D. Zhao, J. Feng, Q. Huo, N. Melosh, G. H. Fredrickson, B. F. Chmelka, G. D. Stucky. *Science*, 1998, **279**, 548–552.

[6] F. Kleitz, S. H. Choi, R. Ryoo, *Chem. Commun.*, 2003, **17**, 2136–2137.

[7] M. Ziolek, I. Nowak, *Zeolites*, 1997, **18**, 356–360.

[8] A. Corma, M. E. Domine, L. Nemeth, S. Valencia, *J. Am. Chem. Soc.*, 2002, **124**, 3194–3195.

[9] W. Fu, R. Shen, E. Bai, L. Zhang, Q. Chen, Z. Fang, G. Li, X. Yi, A. Zheng, T. Tang, *ACS Catal.*, 2018, **8**, 9043–9055.

[10] H. Zhu, A. Ramanathan, J. F. Wu, B. Subramaniam, *ACS Catal.*, 2018, **8**, 4848–4859.

[11] A. Bruehwiler, N. Semagina, M. Grasemann, A. Renken, L. Kiwi-Minsker, A. Saaler, H. Lehmann, W. Bonrath, F. Roessler, *Ind. Eng. Chem. Res.*, 2008, **47**, 6862–6869.

[12] N. Cherkasov, *J. Mol. Liq.*, 2020, **301**, 112378.

[13] C. H. Huang, K. P. Chang, H. D. Ou, Y. C. Chiang, C. F. Wang, *Microporous Mesoporous Mater.*, 2011, **141**, 102–109.